A comparative study on the performances of organic light-emitting diodes with C_{60} and C_{70} cathode buffer layer

WENJIA LI[a,*], LINA SU[a], JIAN REN[a], JIAQI WU[b]
aHuaiyin Normal University, Huaian 223300, China
bSuntech Power Co. Ltd., Wuxi 214028, China

Organic light-emitting diodes based on Alq_3 (8-hydroxyquinoline aluminum) were fabricated using C_{60} and C_{70} as cathode buffer layer, respectively. The results showed that EL performances of OLEDs using C_{70}- buffer-layer were better than that of C_{60}- buffer-layer. The mechanisms of enhancement were systemically discussed on the energy level difference of the heterojunction, conductivity of the materials and electron transport and quantum current distribution in the two kinds of fullerene molecules. The degradation of the two kinds of OLEDs exposed in air without encapsulation was also studied. It was found that OLEDs using C_{70} as cathode buffer layer showed a better stability. This is because C_{60} can be easily destroyed by oxygen than C_{70}. Thus, C_{70} cathode buffer layer can not only increase the EL characteristics, but also dramatically improve the stability of OLEDs.

1. Introduction

Since Tang [1] reported the first Alq_3-based multilayer electroluminescent devices in 1987, organic light-emitting diodes (OLEDs) have attracted a great deal of attention because of light weight, quick response and simple manufacturing technique [2-3]. Nowadays, OLEDs have been successfully applied on commercial panel displays, mobile phones and televisions, and are expected to become the next generation of solid-state luminescence technology.

Over the years, researchers have developed a variety of luminescent materials to achieve the OLEDs of various colors such as blue [4-6], red [5], yellow [7], white [6,8] and so on. Meanwhile, many new structures, such as inverted top-emitting OLEDs [9], tandem OLEDs [10], are investigated to improve the OLEDs performance. Besides, the stability of OLEDs has also been greatly concerned. Based on the study of aging mechanism [11-12], desiccant film [13], Al_2O_3 film [14] and surface-modified nanoclay composite [15] were proposed to encapsulate the OLEDs, which could effectively suppress attenuation.

However, improving the luminescent efficiency of OLEDs occupies the dominant position over the research. Firstly, luminescent materials were modified, for example graphene oxide [16] and TiO_2 [17] were doped into the emitting layer (EML) Alq_3. Moreover new electrodes were developed, for instance, cathode with corrugated nanostructures [18], AgNW/PEDOT:PSS film treated by hot-pressing as electrode [19], ITO-free ultra-thin silver electrode [20] and so on. In addition, advanced anode modification layers were employed such as pyrimidine based hole-blocking materials [21], fluorene/indole-based hole transport materials [22] and MoO_3 anodic buffer layer [23].

Similarly, cathode modification can also enhance efficiency, which is more remarkable for OLEDs where Alq_3 acts as both EML and electron transport layer (ETL). This is because the hole mobility of TPD (a typical hole transport material) is about $10^{-3} cm^2 \cdot V^{-1} \cdot s^{-1}$[24], which is two orders of magnitude higher than the electron mobility of Alq_3 (about $10^{-5} cm^2 \cdot V^{-1} \cdot s^{-1}$[24]). Thus the ability of electron injection from Al cathode to Alq_3 EML is very poor, resulting in unsatisfactory optical output and undesirable luminescent efficiency. Therefore it is very important to achieve a balance between electrons and holes by inserting electron injection layers, electron transportation layers or hole blocking layers between EML and cathode.

C_{60}, which is a common acceptor material in small molecule and polymer cells, was used as anode [25-29] or cathode [29] buffer layer in OLEDs or tandem OLEDs [30]. C_{70}, another member of fullerene, is similar to C_{60}. But OLEDs using C_{70}-buffer-layer were rarely reported. In this paper, C_{70} is used as a cathode buffer layer instead of C_{60}. And the mechanisms of the enhancement of OLEDs are systemically discussed. Also the degradations of OLEDs using C_{60} or C_{70} as cathode buffer layer exposed in

air without encapsulation are studied. It is found that OLEDs using C_{70} cathode buffer layer show a better stability.

2. Experimental

OLEDs with area about 0.06 cm^2 are fabricated in a typical sandwich structure: ITO/TPD/Alq$_3$/C$_{60}$/Al (Device A) and ITO/TPD/Alq$_3$/C$_{70}$/Al (Device B). 7Ω/□ ITO (Indium-Tin Oxide)-glass substrates are sequentially cleaned by ultrasonic treatment in acetone, isopropyl alcohol and deionized water, blown by N$_2$ gas, and treated by UV–Ozone for 15 min. The UV wavelength used here is 185 nm. The power of the UV lamp is 20W, which is put in an airtight box with the capacity of about 40 L. Ozone gas is generated by UV light which excites oxygen in air inside the box. The temperature and humidity inside the box are always kept at 20°C and 30%, respectively.

The purity of C$_{60}$ and C$_{70}$ is 99.9%+, and they are not further purified before experiments. All the organic layers in OLEDs are fabricated by vacuum evaporation at a pressure of 4.0×10^{-3} Pa, while Al at 2.0×10^{-3} Pa. Thicknesses are 20, 20, 1 and 100 nm for TPD, Alq$_3$, C$_{60}$ (or C$_{70}$) and Al, respectively. The thicknesses of the layers are monitored by a quartz oscillator thickness monitor and they are also checked by an ellipsometer (produced by Gaertner Scientific Corporation).

The current–voltage (J–V) and luminance-current (L-J) characteristics and the stability of OLEDs are measured with LED620 intensity distributing test meter, while the spectra characteristics are obtained from PMS-50(PLUS) UV-Vis-nearFR spectrophotocolorimeter (both of them are produced by Everfine Photo-E-Information CO., LTD). The stabilities of the conductivity of C$_{60}$ and C$_{70}$ films have been measured by Keithley 2400 sourcemeter in our previously work [31].

3. Result and discussion

3.1. J-V characteristics

The J-V and L-J curves of OLEDs with C$_{60}$ (or C$_{70}$) buffer layer inserted at Alq$_3$/Al interface are presented in Table 1 and Fig. 1. The data were recorded immediately after the devices removing from the vacuum system.

Table 1. Luminescent parameters for the devices (the leakage current was measured with working current 2.20mA)

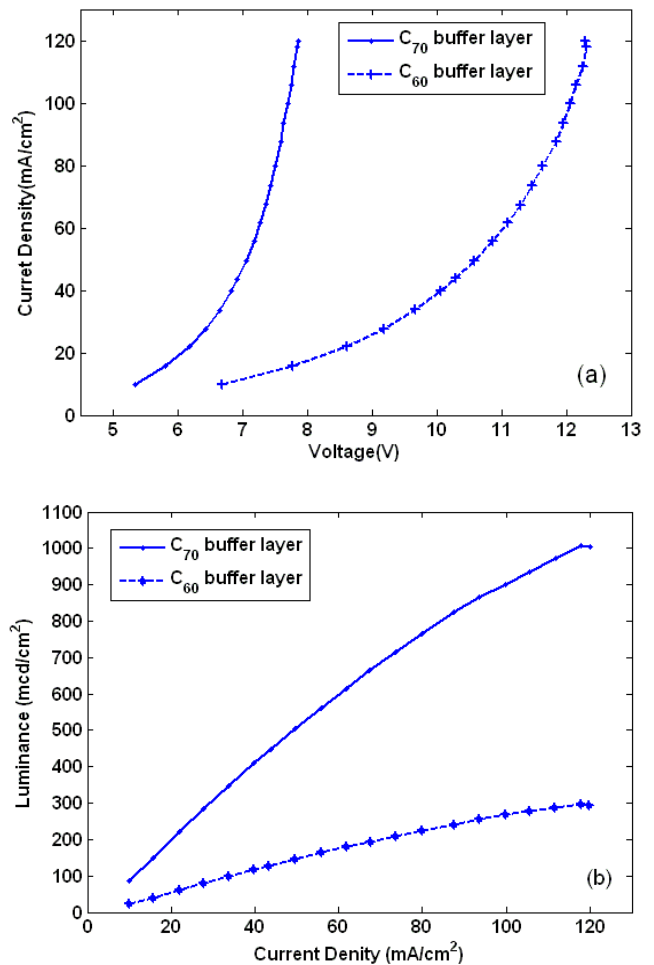| Structure	Leakage Current (μA)	Driving Voltage (V)	Efficiency (lm/W)
ITO/TPD/Alq$_3$/C$_{60}$/Al	0.58	6.69	6.79
ITO/TPD/Alq$_3$/C$_{70}$/Al	0.18	5.35	10.12

Fig. 1. Characteristics of the OLEDs with C_{60} and C_{70} cathode buffer layers inserted at the Alq$_3$/Al interface. (a) and (b) show the current density vs. voltage (J–V) and the luminance vs. current density (L–J) properties, respectively

The two devices have the same structure, as shown in Fig. 2. The only difference is focused on the buffer layer. However, it is clear that the behavior of device A is much inferior to that of device B.
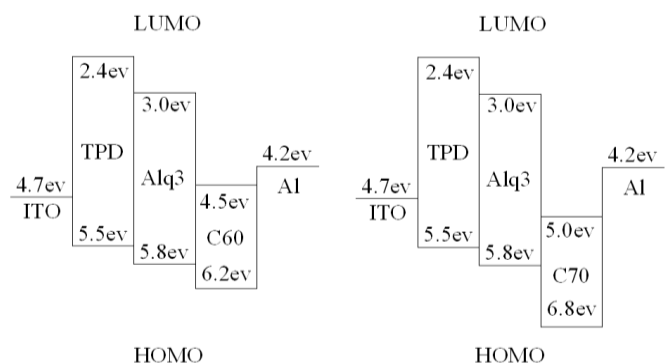

Fig. 2. Schematic energy-level diagram of devices

Firstly, device B shows a higher current density at the same voltage (Fig. 1a) and an increased luminance at the same current density (Fig. 1b). The device current density J_s and the luminescence power can be expressed by the following equations [32]:

$$J_s = J_e + J_h^{'} = J_h + J_e^{'} \qquad (1)$$

$$P_{EL} \propto J_e - J_e^{'} = J_h - J_h^{'} \qquad (2)$$

where J_e and J_h are the current densities of injected electrons and holes from the cathode and anode, respectively, and J'_e and J'_h are the fraction of electron and hole current densities reaching the counter electrode without recombination. According to Song et al. [26], as there was no difference in electron injection, the increase of J_s should be due to the decrease of J'_e, which means the leakage current is decreased. The leakage currents have been measured and are shown in Table 1. Device A has a leakage current 0.58μA which is three times that of device B.

The reason of the lower leakage current of device B is that the HOMO of C_{70} (6.8eV) is much lower than that of C_{60} (6.2eV), which leads to an effective block of holes. As the brightness and efficiency properties of OLEDs greatly depend on the balance of charge carrier [33-35], C_{70} which has a stronger ability of hole blocking than C_{60} would drive the carriers to reach a better balance, and then, a higher current density and EL intensity are obtained. Here C_{60} and C_{70} act as hole blocking layers. The fewer holes reach the cathode, the lower leakage current can be measured. Device B can more effectively utilize the injection holes which cause an enhancement of current density and output luminance.

Additionally, the different electron transport and quantum current distribution inside the molecules of C_{60} and C_{70} also influence the current density of the devices. C_{60} can absorb six electrons per molecule and it can play a role of electron trapping center [36]. The fraction of electrons injected from cathode can be captured and deactivated by C_{60} molecule [36]. Wang et al. [37-38] have studied this issue, and found that there are many circulating circuits in C_{60} molecule when carriers transported into it, whereas none has been seen in C_{70} molecule (see Fig. 3). Wang et al. [37] also state that the quantity of the electrons output from C_{60} molecule is smaller than the input quantity, while these two quantities are the same in C_{70} molecule. Thus more carriers and excitons will be recombined in C_{60} layer, and cause a lower current density of OLEDs.
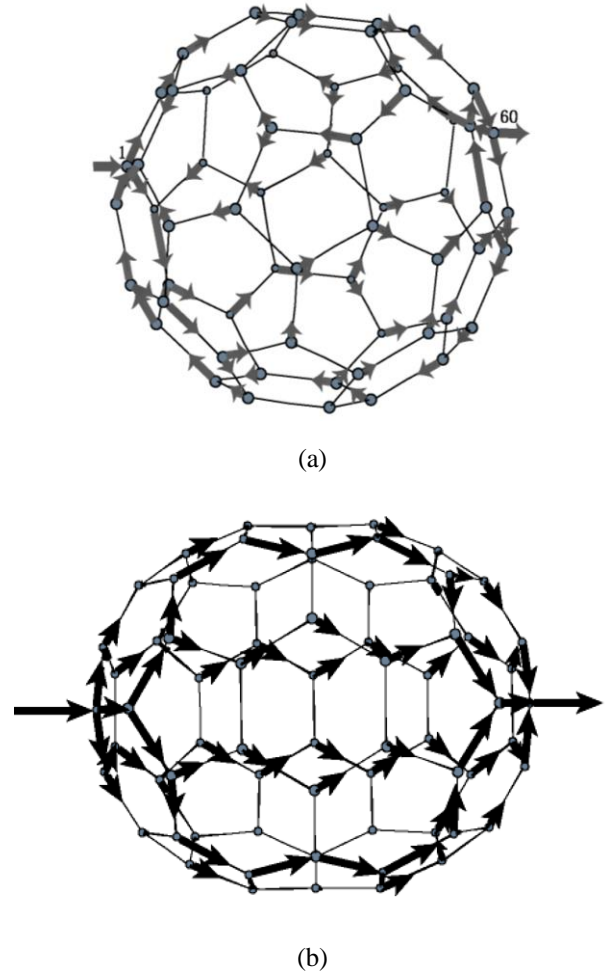

(a)

(b)

Fig. 3 (a) Electron transport and quantum current distribution of C_{60} molecule [37]. (b) Electron transport and quantum current distribution of C_{70} molecule [38].

In other respects, the conductivities of C_{60} and C_{70} are listed in Table 2 which have been measured in our previously work [31]. It is obvious that the values of C_{70} are always two orders higher than those of C_{60} (no matter at the condition of dark or illumination). A higher conductivity corresponds to a lower series resistance for the device, and it offers a higher current density at the same voltage.

Table 2. Conductivity values of C_{60} and C_{70} at dark conduction and an illumination of 100 mW/cm^2 with an AM1.5G sun simulator [31]

Material	Dark (S/cm)	AM1.5G (S/cm)
C_{60}	$7.8×10^{-15}$	$9.36×10^{-14}$
C_{70}	$9.6×10^{-13}$	$5.91×10^{-12}$

As can be seen in Table 1, device B has a smaller driving voltage than that of device A. Generally, a reduced carrier injection barrier could cause the drop of driving voltage [39]. But the LUMO of C_{70} is 0.5eV lower than that of C_{60} as shown in Fig. 2, which further added the injection barrier between Alq_3 and Al. The reasons are still unclear. This phenomenon could not only ascribe to the effect of using a simplified energy band model. A possible factor may be the different electron transport and quantum current distribution inside the two molecules. It has been mentioned above, C_{60} recombines more carriers and excitons. To prevent the recombination, more electrical pressure is required to defend against such a large recombination velocity inside C_{60} layer, which results in a higher driving voltage.

With higher current density and lower leakage current and driving voltage, device B eventually presents a more favorable efficiency (about 1.5 times of device A) as indicated in Table 1.

3.2. Degradation

The stabilities of OLEDs without encapsulation are shown in Fig. 4. The luminance was measured by LED620 intensity distributing test meter every 10 seconds and normalized to their initial values. The devices were always placed in the aphotic test meter during the measurement process where the temperature was kept at 25°C and the humidity was kept below 15%.
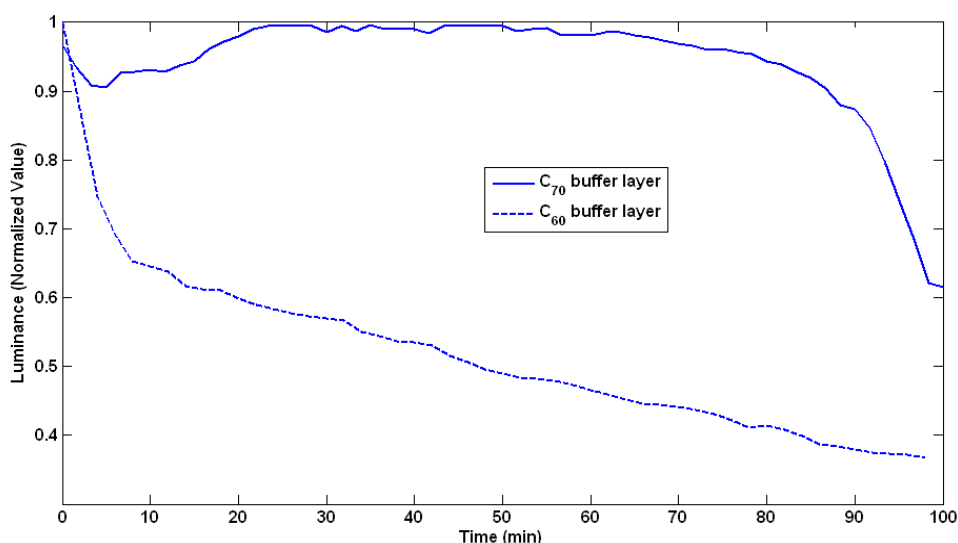

Fig. 4. The degradations of the OLEDs using C_{70}-buffer-layer and C_{60}-buffer-layer in air-exposure without encapsulation

OLEDs which is exposed to atmosphere directly and without encapsulation, have limited lifetime: operating OLEDs in air resulted in a 99% loss of EL intensity in as little as 150 min [40]. In this work, what our concern is the different attenuation trends of the two kinds of devices. Because how long OLEDs will stably operate without encapsulation is not the emphasis here, Fig. 4 only displays the stabilities during the first 100 minutes after fabrication. It is obvious that the stability of device B with C_{70} buffer layer is much better than that of device A, which has the same result with thin film transistors (TFTs) using C_{70} [41] and C_{60} [42] and organic solar cells with C_{70} and C_{60} acting as acceptor [31]. Meanwhile, the degradation curve of device B is attractive because the luminance was enhanced a little during the first 60 minutes after fabrication.

Popularly, there are complex intrinsic mechanisms which contribute to the degradation process: migration of mobile ions [43], injection of holes into Alq_3 [44-45],

crystallization of Alq_3 layers or the delamination at the cathode Alq_3 interface [46–48], gas evolution from galvanic corrosion of Mg/Ag cathode [49] and morphological changes in electrode [50]. But it is proposed that the more important factors are environmental factors such as light, oxygen and humidity [51].

In order to improve the understanding of degradation process, it is useful to study the stability of materials and thin films separately, followed by study of efficiency and stability of OLEDs [52]. In this case, to explain the difference between two devices in this paper, stabilities of C_{60} and C_{70} buffer layer must be compared.

The stabilities of the dark conductivity of C_{60} and C_{70} films exposed in air were studied in our previously work [31]. Fig. 5 shows the degradations of the normalized conductivity of C_{60} and C_{70} films exposed in air. It is clear that the conductivity degradation of C_{60} is much more and faster than that of C_{70}.
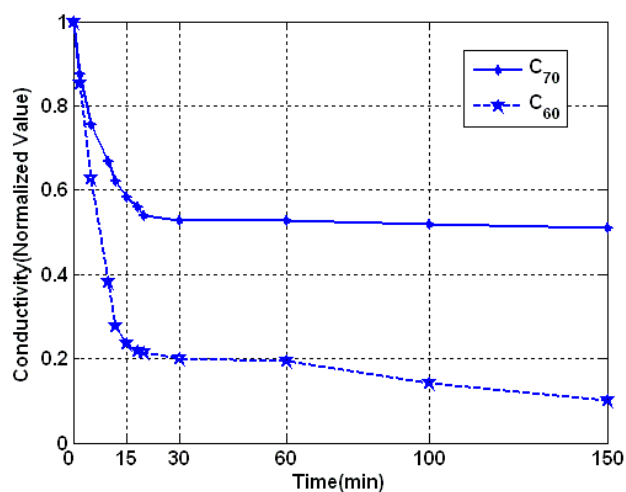
Fig. 5. The degradations of the conductivities of C_{60} and C_{70}
films exposed in the air under dark condition [31]

Because the humidity in the lab was kept below 15% and devices were always put in the aphotic test meter during the measurement process, oxygen becomes the major factor causing the degradation. Oxygen molecules act as electron traps in the lattice of fullerene molecules [42]. More oxygen molecules infiltrate into the buffer layer, more electrons will be recombined, and fewer carriers can arrive at the active EL layer, then performances of the device will get worse.

Device B has a better performance ascribing to the better stability of C_{70}. The higher electron affinity and ionization potential of C_{70} can be effective in delocalizing the carriers, and thereby preventing the formation of deep traps by lattice relaxation [41]. In addition, because of the lower symmetry of C_{70} than that of C_{60}, the influence to the mobility of the carriers from the additional variable introduced from the circumstance can be seriously impaired in C_{70} film [41]. So less recombined electrons will cause a stable performance of C_{70} and result in a better EL characteristics and a better stability of OLEDs.

As mentioned above, degradation trend of device B get a little raised during the first hour after fabrication, and then begin to decline. The enhancements can be attributed to the appearance of Al_2O_3 layer at the interface of C_{70}/Al, and the function of Al_2O_3 layer is similar to an insulating cathode buffer layer [52]. The deceleration of the formation of "C–Al" [53] can promote an improvement of the stability. However, with the continuous increase in the thickness of the Al_2O_3 layer, more and more electrons will be blocked by a thicker insulating layer, and the electron transmission efficiency will decrease, then the performances start to decline later [54]. But it is regret that stability of device A can not be improved, and the degradation trend of device A is coherent with material C_{60}. As shown in Fig. 5, conductivity of C_{60} declines 60% in 10 min and 80% in 30 min. It is proved that C_{60} layer has

been destroyed by oxygen before Al_2O_3 formed and can not act as a functional buffer layer with time going by.

3.3. Spectra

As shown in Table 3, the EL spectra of devices with C_{60} and C_{70} buffer layers were measured, respectively. Similar spectra were observed and both of them had a peak wavelength at about 505 nm due to the green emission of Alq_3 and an average wavelength at about 515 nm. Therefore, it was found that any energy transfers between C_{60} (C_{70}) and Alq_3 molecules did not occur by inserting C_{60} (C_{70}) ultrathin layers.

Table 3. Spectra parameters for the devices

Structure	Peak WaveL(nm)	Average WaveL (nm)	Purity
ITO/TPD/Alq_3/Al	505	515	34.5%
ITO/TPD/Alq_3/C_{60}/Al	510	517	35.9%
ITO/TPD/Alq_3/C_{70}/Al	505	512	38.1%

4. Conclusion

In this paper, OLEDs with C_{60} and C_{70} cathode buffer layer were studied.

(1) OLEDs using C_{70} buffer layer show higher current density, luminance and efficiency but lower leakage current and driving voltage compared with the ones using C_{60} buffer layer, because of C_{70} molecule's lower HOMO level, higher conductivity and better electron transport and quantum current distribution.

(2) The C_{70}-buffer-layer OLEDs operate more stable than that of C_{60}, which correspond with the stability of C_{70} and C_{60} films' conductivity. This is caused by the higher electron affinity and ionization potential, and the lower symmetry of C_{70}. In addition, characteristics of device using C_{70} get improved during the first hour after fabrication because of an appropriate Al_2O_3 layer.

(3) The EL spectrum of the two different devices is almost the same which indicates that the Forster resonance energy transfer did not take place.

In conclusion, C_{70}, instead of C_{60}, may be another effective cathode buffer layer material for its superior properties.

References

[1] C. Tang, S. Vanslyke, Applied Physics Letters **51**(12), 913 (1987).

[2] S. Raupp, L. Merklein, M. Pathak, P. Scharfer, W. Schabel, Chemical Engineering Science **160**, 113 (2017).

[3] A. Wei, J. Sze, Optics Communications **380**, 394 (2016).

[4] J. Peng, X. Xu, X. Feng, L. Li, Journal of Luminescence **198**, 19 (2018).

[5] C. Liu, Y. Chen, Y. Long, P. Sah, W. Chang, L. Chan, J. Wu, R. Jeng, S. Yeh, C. Chen, Dyes and Pigments **157**, 101 (2018).

[6] W. Li, J. Zhao, L. Li, X. Du, C. Fan, C. Zheng, S. Tao, Organic Electronics **58**, 276 (2018).

[7] H. Li, F. Zhang, J. Cheng, L. Ding, Chinese Journal of Luminescence **37**(1), 38 (2016).

[8] Y. Miao, K. Wang, B. Zhao, L. Gao, P. Tao, X. Liu, Y. Hao, H. Wang, B. Xu, F. Zhu, Nanophotonics **7**, 295 (2018).

[9] H. Zhang, L. Wang, J. Rong, J. Cao, Z. Zhang, X. Jiang, J. Zhang, Chinese Journal of Luminescence **33**(6), 611 (2012).

[10] F. Angel, R. Gao, J. Wallace, C. Tang, Organic Electronics **59**, 220 (2018).

[11] P. Weijer, K. Lu, R. Janssen, S. Winter, H. Akkerman, Organic Electronics **37**, 155 (2016).

[12] G. Mao, Z. Wu, Q. He, B. Jiao, G. Xu, X. Hou, Z. Chen, Q. Gong, Applied Surface Science **257**, 7394 (2011).

[13] J. Liu, F. Zhang, Chinese Journal of Luminescence **38**(1), 76 (2017).

[14] W. Duan, S. Li, H. Zhang, Z. Zhang, J. Zhang, Chinese Journal of Luminescence **37**(1), 88 (2016).

[15] D. Kang, G. Park, H. Park, J. Park, H. Im, Progress in Organic Coatings **118**, 66 (2018).

[16] S. Guo, X. Du, X. Liu, H. Liu, H. Wang, Y. Hao, B. Xu, J. Zhao, K. Guo, Chinese Journal of Luminescence **34**(5), 595 (2013).

[17] W. Li, C. Wu, Y. Miao, Y. Li, H. Wang, K. Guo, Chinese Journal of Luminescence **36**(2), 219 (2015).

[18] Y. Liu, M. An, X. Zhang, Y. Bi, D. Yin, Y. Zhang, J. Feng, H. Sun, Applied Physics Letters **109**(19), 193301 (2016).

[19] B. Wei, X. Wu, L. Lian, S. Yang, D. Dong, D. Feng, G. He, Organic Electronics **43**, 182 (2017).

[20] G. Kumar, Y. Li, S. Biring, Y. Lin, S. Liu, C. Chang, Organic Electronics **42**, 52 (2017).

[21] S. Jang, S. Han, J. Lee, Y. Lee, Synthetic Metals **239**, 43 (2018).

[22] N. Xiang, Z. Gao, G. Tian, Y. Chen, W. Liang, J. Huang, Q. Dong, W. Wong, J. Su, Dyes and Pigments **137**, 36 (2017).

[23] F. Dong, R. Ding, S. Hotta, A. Li, Optics Communications **392**, 247 (2017).

[24] C. Huang, F. Li, W. Huang, Introduction to Organic Light-Emitting Materials and Devices, Fudan University Press, Shanghai, 2005.

[25] Z. Lv, Z. Deng, J. Zheng, Y. Yin, Y. Chen, Y. Wang, Physica B **405**, 335 (2010).

[26] D. Song, S. Zhao, F. Zhang, Z. Xu, J. Li, X. Yue, H. Zhu, L. Lu, Y. Wang, Journal of Luminescence **129**, 1978 (2009).

[27] K. Kato, K. Takahashi, K. Suzuki, T. Sato, K. Shinbo, F. Kaneko, H. Shimizu, N. Tsuboi, T. Tadokoro, S. Ohta, Current Applied Physics **5**, 321 (2005).

[28] Q. Song, C. Li, M. Wang, X. Sun, Thin Solid Films **516**, 8675 (2008).

[29] Z. Lv, Z. Deng, D. Xu, X. Li, Y. Jia, Displays **30**, 23 (2009).

[30] Z. Lv, X. Li, Y. Wang, J. Xiao, P. Xu, Current Applied Physics **14**, 1465 (2014).

[31] X. Xi, W. Li, J. Wu, J. Ji, Z. Shi, G. Li, Solar Energy Materials and Solar Cells **94**, 2435 (2010).

[32] D. Liu, M. Fina, Z. Chen, X. Chen, G. Liu, S. Johnson, S. Mao, Applied Physics Letters **91**, 093514 (2007).

[33] D. Liu, F. Teng, Z. Xu, S. Yang, L. Qian, Q. He, Y. Wang, X. Xu, Journal of Luminescence **122-123**, 656 (2007).

[34] R. Meeheim, S. Scholz, S. Olthof, G. Schwartz, S. Reineke, K. Walzer, K. Leo, Journal of Applied Physics **104**, 014510 (2008).

[35] D. Zhao, X. Sun, C. Jiang, A. Kyaw, G. Lo, D. Kwong, Applied Physics Letters **93**, 083305 (2008).

[36] J. Lee, Synthetic Metals **156**, 852 (2006).

[37] L. Wang, D. Yu, Y. Li, M. Tsukada, Journal of Synthetic Crystals **34**, 637 (2008).

[38] L. Wang, Y. Li, D. Yu, M. Tsukada, Science China G: Physica, Mechanica, Astronomica **37**, 576 (2007).

[39] Y. Park, J. Jang, Y. Kim, J. Choi, T. Park, J. Choi, B. Ju, Thin Solid Films **517**, 4108 (2009).

[40] Y. Hamada, C. Adachi, T. Tsutsui, S. Saito, Japanese Journal of Applied Physics **31**, 1812 (1992).

[41] R. Haddon, Journal of the American Chemical Society **118**, 3041 (1996).

[42] R. Haddon, A. Perel, R. Morris, T. Palstra, A. Hebard, R. Fleming, Applied Physics Letters **67**, 121 (1995).

[43] J. Shen, D. Wang, E. Langlois, W. Barrow, P. Green, C. Tang, J. Shi, Synthetic Metals **111-112**, 233 (2000).

[44] Z. Popovic, H. Aziz, IEEE Journal of Selected Topics in Quantum Electronics **8**, 362 (2002).

[45] Z. Popovic, H. Aziz, N. Hu, A. Ioannidis, P. Anjos, Journal of Applied Physics **89**, 4673 (2001).

[46] P. Burrows, V. Bulovic, S. Forrest, L. Sapochak, D. McCarty, M. Thompson, Applied Physics Letters **65**, 2922 (1994).

[47] Z. Popovic, S. Xie, N. Hu, A. Hor, D. Fork, G. Anderson, C. Tripp, Thin Solid Films **363**, 6 (2000).

[48] H. Aziz, Z. Popovic, S. Xie, A. Hor, N. Hu, C. Tripp, G. Xu, Applied Physics Letters **72**, 756 (1998).

[49] H. Aziz, Z. Popovic, C. Tripp, N. Hu, A. Hor, Applied Physics Letters **72**, 2642 (1998).

[50] L. Do, M. Oyamada, A. Koike, E. Han, N. Yamamoto, M. Fujihira, Thin Solid Films **273**, 209 (1996).

[51] S. Zardareh, F. Boroumand, World Academy of Science, Engineering and Technology **50**, 274 (2009).

[52] C. Kwong, A. Djurisic, W. Choy, D. Li, M. Xie, W. Chan, K. Cheah, P. Lai, P. Chui, Materials Science and Engineering B **116**, 75 (2005).

[53] M. Jørgense, K. Norrman, F. Krebs, Solar Energy Materials and Solar Cells **92**, 686 (2008).

[54] X. Xi, F. Li, Q. Meng, Y. Ding, J. Ji, Z. Shi, G. Li, Solar Energy Materials and Solar Cells **94**, 924 (2010).

_____

*Corresponding author: liwenjia0921@foxmail.com